Mansoura Engineering Journal, (MEJ), Vol. 38, No 2, June 2013 E. 15

A three-phase induction motor performance under different loading types supplied from balanced and unbalanced Thyristorized supply voltage

أداء المحرك التأثيري الثلاثي الاوجه تحت أنواع مختلفه من التحميل المغذي من منبع جهد خلال ثيرستورات متزنه وغيرمتزنه

A. S. Hassan , A. R. A. Amin[1] and A. Farahat[2]

1 Professor of Power Electronics

2 Doctor of Electrical Machines

Dept.of Electrical Engineering

Faculty of Engineering

Mansoura University

الخلاصه:

تستخدم المحركات التأثيريه في العديد من التطبيقات الصناعيه وأدي التطور في مجال الكترونيات القوي الي زياده استخدام مفاتيح الثيرستور للتحكم في جهد تغذيه المحركات التأثيريه بغرض التحكم في السرعه واليدء الناعم وتوفير الطاقه في هذه التطبيقات . وهذه المفاتيح تؤدي الي تغذيه المحركات التأثيريه بأشكال متعدده من موجات الجهد الغيرجيبيه طبقا لتشغيل الثيرستورات بشكل متزن وغير متزن . لذلك فان هذا البحث يتناول تأثيرشكل موجه جهد التغذيه الغيرجيبي علي الاداء الديناميكي للمحركات التأثيريه عند التشغيل المتزن والغيرمتزن وكذلك عند ظروف التحميل المختلفه. وقد تم تمثيل اداء المحرك التأثيري المغذي من خلال الثايرستور ببرنامج MATLAB.

Abstract:

Induction motors are used extensively in a wide variety of industrial applications. The developments in the power electronics field have lead to an ever- increasing use of thyristors switching devices in the induction motors supply voltage control for the purpose of speed control, soft starting, and energy saving in these applications . Such power electronics switching devices generate different waveforms patterns of nonsinusoidal voltage according to balanced and unbalanced condition of their operation. So, The present paper investigates the impact of this nonsinusoidal supply voltage waveforms on the dynamic performance of a three-phase induction motor during balanced and unbalanced operation. Also, this paper considers the IM operation at different loading conditions. A MATLAB program has been used to model the thyristorized induction motor performance.

Accepted: June, 30, 2013

I-Introduction

Polyphase induction motors have been the workhorse (main prime movers) for many industrial applications. In some of these applications, thyristor switching devices, are often employed as effective and low-cost means for voltage control of the induction motor for the purpose of speed control, soft starting, and energy saving.

The application of thyristors to supply the induction motor has resulted in a number of nonsinusoidal supply voltages according to their switching mode of operation. Although induction motors (IMs) are generally operated under balanced conditions, various unbalanced or unsymmetrical conditions can occur. For example, the stator phase voltages may become temporarily unbalanced due to faults occurring in thyristor switching devices.

Such Induction motor–electronic switching devices can be found in applications that involve numerous load systems such as fans, blowers, compressors, centrifugal pumps, elevators and escalators, assembly lines, transport and conveyor-belt systems, as well as heating, ventilation, and air conditioning (HVAC) systems. In these vital and critical applications, the study of the impacts of the balanced and unbalanced supply voltage on the dynamic performance of IM is very important.

Many studies have been reported about the influence of supply voltage on the induction motor operation [1]-[14]. The dynamic performance of the unloaded IM under a balanced sinusoidal voltage source was proposed and the effects of various unbalanced and unsymmetrical conditions for the voltage source on it were investigated [1]-[2]. Berge [15], [16] studied the dynamic performance of IM loaded by pump load when it is supplied through thyristors based stator voltage control. However, an important issue weren't considered and discussed in the previous researches, is the impact of the supply voltage waveforms with different loading types on the dynamic performance of IM. Therefore, this paper provides an extensive investigation for the following problems:

1)-The dynamic performance of the motor in the form of a sinusoidal operation on the supply side under both balanced and unbalanced conditions at different loading conditions.

2)-The dynamic performance of the motor when used in conjunction with thyristors switching devices under both balanced and unbalanced conditions at different loading conditions .

II. Mathematical Model of induction motor

The mathematical model of the IM in terms of ABC/abc axes quantities is used. Given in reference [17], [18], the voltage equations describing an induction motor are:

$$v_{abcs} = r_s i_{abcs} + p\lambda_{abcs} \quad (1)$$

$$v_{abcr} = r_r i_{abcr} + p\lambda_{abcr} \quad (2)$$

For a magnetically linear system, the flux linkages may be expressed as

$$\begin{bmatrix}\lambda_{abcs}\\ \lambda_{abcr}\end{bmatrix} = \begin{bmatrix} L_s & L_{sr} \\ (L_{sr})^T & L_r \end{bmatrix}\begin{bmatrix} i_{abcs} \\ i_{abcr}\end{bmatrix} \quad (3)$$

When expressing the voltage equations in machine variable form, it is convenient to refer all rotor variables to the stator windings by appropriate turns ratios:

$$\lambda'_{abcr} = \frac{N_s}{N_r}\lambda_{abcr}$$

$$, i'_{abcr} = \frac{N_r}{N_s} i_{abcr} , \qquad L'_r = (\frac{N_s}{N_r})^2 L_r \quad (4)$$

$$\begin{bmatrix}\lambda_{abcs}\\ \lambda'_{abcr}\end{bmatrix} = \begin{bmatrix} L_s & L'_{sr} \\ (L'_{sr})^T & L'_r \end{bmatrix}\begin{bmatrix} i_{abcs} \\ i'_{abcr}\end{bmatrix} \quad (5)$$

The voltage equations expressed in terms of machine variables referred to the stator windings may now be written as

$$\begin{bmatrix}v_{abcs}\\ v'_{abcr}\end{bmatrix} = \begin{bmatrix} r_s + pL_s & pL'_{sr} \\ p(L'_{sr})^T & r'_r + pL'_r \end{bmatrix}\begin{bmatrix} i_{abcs} \\ i'_{abcr}\end{bmatrix} \quad (6)$$

Where

$$L_s = \begin{bmatrix} L_{ms} + L_{ls} & -\frac{L_{ms}}{2} & -\frac{L_{ms}}{2} \\ -\frac{L_{ms}}{2} & L_{ms} + L_{ls} & -\frac{L_{ms}}{2} \\ -\frac{L_{ms}}{2} & -\frac{L_{ms}}{2} & L_{ms} + L_{ls} \end{bmatrix}$$

$$L'_r = \begin{bmatrix} L_{ms} + L'_{lr} & -\frac{L_{ms}}{2} & -\frac{L_{ms}}{2} \\ -\frac{L_{ms}}{2} & L_{ms} + L'_{lr} & -\frac{L_{ms}}{2} \\ -\frac{L_{ms}}{2} & -\frac{L_{ms}}{2} & L_{ms} + L'_{lr} \end{bmatrix}$$

$$L'_{sr} = \begin{bmatrix} L_{ms}\cos\theta_r & L_{ms}\cos\left(\theta_r + \frac{2\pi}{3}\right) & L_{ms}\cos\left(\theta_r - \frac{2\pi}{3}\right) \\ L_{ms}\cos\left(\theta_r - \frac{2\pi}{3}\right) & L_{ms}\cos\theta_r & L_{ms}\cos\left(\theta_r + \frac{2\pi}{3}\right) \\ L_{ms}\cos\left(\theta_r + \frac{2\pi}{3}\right) & L_{ms}\cos\left(\theta_r - \frac{2\pi}{3}\right) & L_{ms}\cos\theta_r \end{bmatrix}$$

$$\begin{bmatrix} v_{abcs} \\ v'_{abcr} \end{bmatrix} = \begin{bmatrix} r_s \\ r'_r \end{bmatrix} \begin{bmatrix} i_{abcs} \\ i'_{abcr} \end{bmatrix} + p\left(\begin{bmatrix} L_s & L'_{sr} \\ (L'_{sr})^T & L'_r \end{bmatrix} \begin{bmatrix} i_{abcs} \\ i'_{abcr} \end{bmatrix} \right) \quad (7)$$

$$\begin{bmatrix} v_{abcs} \\ v'_{abcr} \end{bmatrix} = \begin{bmatrix} r_s \\ r'_r \end{bmatrix} \begin{bmatrix} i_{abcs} \\ i'_{abcr} \end{bmatrix} + p\left(\begin{bmatrix} i_{abcs} \\ i'_{abcr} \end{bmatrix} \right) \begin{bmatrix} L_s & L'_{sr} \\ (L'_{sr})^T & L'_r \end{bmatrix} + \begin{bmatrix} i_{abcs} \\ i'_{abcr} \end{bmatrix} p\left(\begin{bmatrix} L_s & L'_{sr} \\ (L'_{sr})^T & L'_r \end{bmatrix} \right) p(\theta_r) \quad (8)$$

So, $p\left(\begin{bmatrix} i_{abcs} \\ i'_{abcr} \end{bmatrix} \right) =$

$$\begin{bmatrix} L_s & L'_{sr} \\ (L'_{sr})^T & L'_r \end{bmatrix}^{-1} \left(\begin{bmatrix} v_{abcs} \\ v'_{abcr} \end{bmatrix} - \begin{bmatrix} r_s \\ r'_r \end{bmatrix} \begin{bmatrix} i_{abcs} \\ i'_{abcr} \end{bmatrix} - \begin{bmatrix} i_{abcs} \\ i'_{abcr} \end{bmatrix} p\left(\begin{bmatrix} L_s & L'_{sr} \\ (L'_{sr})^T & L'_r \end{bmatrix} \right) p(\theta_r) \right) \quad (9)$$

And the electromagnetic torque can be expressed as

$$T_e = \left(\frac{P}{2}\right) (i_{abcs})^T \frac{\partial}{\partial \theta_r} [L'_{sr}] i'_{abcr} \quad (10)$$

The mechanical part is represented by the following equation

$$T_e = Jp\omega_m + f\omega_m + T_L \quad (11)$$

Where J is the moment of inertia, f friction and windage coefficient, ω_m the mechanical motor speed, and T_L the shaft load torque.

III-proposed Procedure:

This paper investigates the dynamic performance of motor electromagnetic torque, speed and supply currents for operation on sinusoidal and non-sinusoidal under both balanced and unbalanced conditions at different loading conditions.

The proposed procedure is applied using the following steps

1)-First case (sinusoidal operation)

The IM is connected directly to three-phase sinusoidal supply under the following conditions:

a)-Balanced condition

b)-Unbalanced condition

the unbalanced condition considered in this paper is opening one phase of the stator phases of IM under the following loading conditions [19]:

a)-No-load(Free acceleration)

b)-Constant torque load in which the load torque remains constant over a given speed range such as conveyors, augers, reciprocating compressors, crushers and elevators.

c)- Variable torque load in which the load torque varies either linearly with speed such as calenders, paper and textile glazing, and eddy-current brakes or with the square of the speed such as centrifugal pumps, centrifugal fans, centrifugal blowers, vehicles and centrifugal compressors.

d)- Pulsed or transient load in which sudden impact peak load on the motor shaft, usually involves sharp, abrupt changes in load which are not dependent on speed. Impact loads may be non-cyclic in nature.

(2)-Second case (non-sinusoidal operation)

The IM is connected to three-phase sinusoidal supply through two thyristors connected in reverse parallel to each phase. The schematic diagram of the thyristorized IM is given in Fig.1 .It is composed of three pairs of back-to-back connected thyristors (A1,A2,B1,B2,C1,C2) in series with each phase of the motor's stator phase windings. Both the stator winding voltage and motor currents have different nonsinusoidal waveforms that depend on the triggering angle and the load impedance.

The non-sinusoidal operation is carried out under the following condition

a)-Balanced condition

b)-Unbalanced condition

Two distinct types of unbalanced conditions considered in this work are:

(1) short-circuit thyristor fault , and

(2) open-circuit thyristor fault,

This is investigated under the above loading conditions.

IV- Matlab Model of the System

Using the mathematical model developed in II, A three-phase induction motor is modeled using Matlab software [21] .

The validity of the model at sinusoidal and nonsinusoidal operation of the IM was checked with previous works [1],[15],[16]. The results obtained from the model were in complete agreement with their results. So, the model can be applied with sufficient certainty.

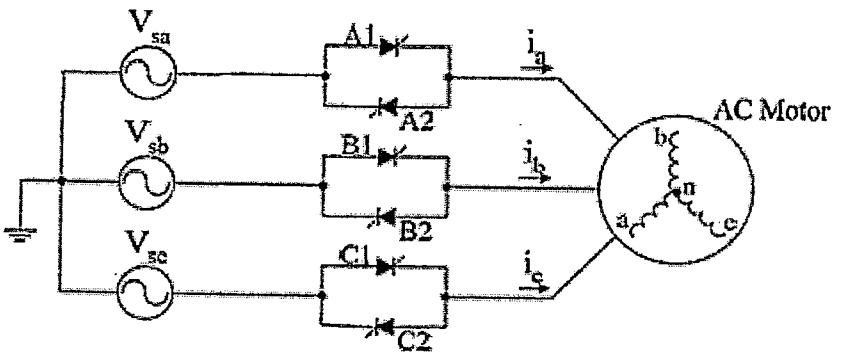

Fig.1 Thyristorized Induction Motor

V- Simulation results:

Simulation results on the dynamic performance of IM were obtained for a three-phase induction motor, the equivalent circuit parameters of which, given in Appendix (A). Two simulation cases were conducted, namely: 1)-Sinusoidal operation, 2)-Non-sinusoidal operation at different loading conditions such as 1)-Free acceleration (no-load), 2)-constant load $T_L = 20$ Nm =full load torque,3)-Pump load $T_L = K_L \omega_m^2$ N. m Where K_L is the Load coefficient and equal to $0.88042 * 10^{-3}$ N. m/(rad/s)^2 which was used to

Provide a mechanical load torque of 20 N.m at the rated speed, and

4)-Pulsed load in which average load torque applied equal to rated load torque 20 Nm .

1)-Sinusoidal operation

the dynamic performance of motor electromagnetic torque, speed and supply currents under the balanced sinusoidal voltage condition are shown in Fig.2, Fig.3, Fig.4 and Fig.5 with different loading types.

the unbalanced operation of IM considered in this paper is the phase-c of the induction motor is disconnected from the supply at time (t=0.41) at that voltage passes through zero going positive, and then reconnected after five cycles from the disconnection time.Fig.6, Fig.7, Fig.8 and fig.9 shows the dynamic characteristics of the induction motor under this condition with different loading types.

2)-Nonsinusoidal operation

In this case, The IM is connected to three-phase sinusoidal supply through thyristors connected in series with three phases (three-leg thyristorized IM) .The continuity of the motor line current waveform is dictated by the setting of firing angle. For

the discontinuous the line current, the firing angle should be greater than the critical angle "σ" which is found to be 63° and 65° for the low voltage and medium voltage IMs respectively [20], so we take the firing angle of thyristors "α" equal to 70° .the dynamic characteristics of the motor under the balanced non-sinusoidal voltage condition are shown in Fig.10, Fig.11, Fig.12 and Fig.13.

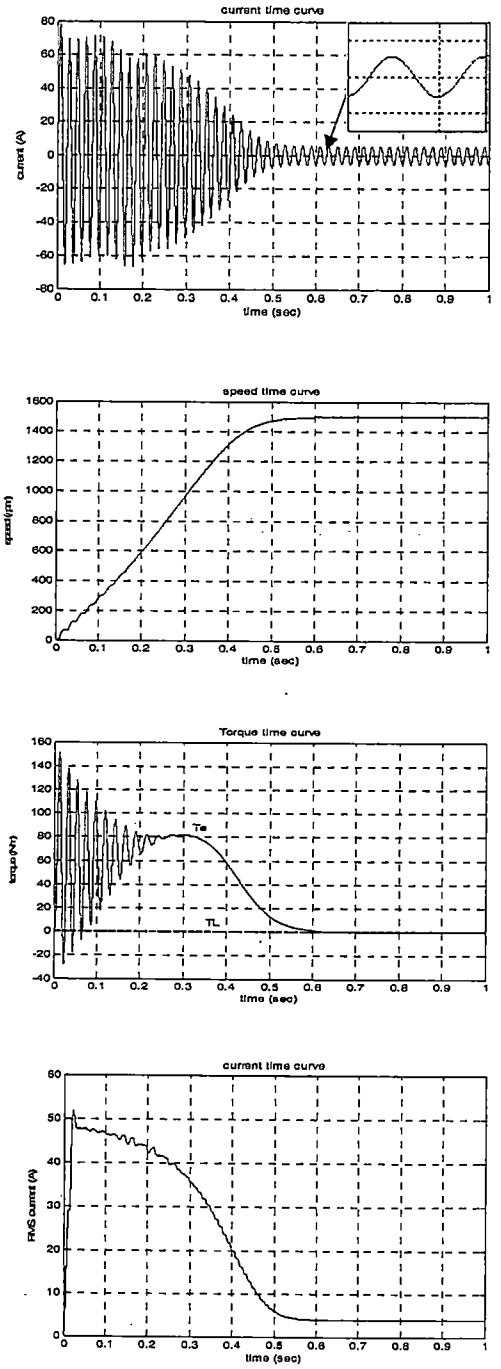

Fig.(2),Transient current, Speed,Torque , and RMS current vs time for balanced sinusoidal operation at no- load application.

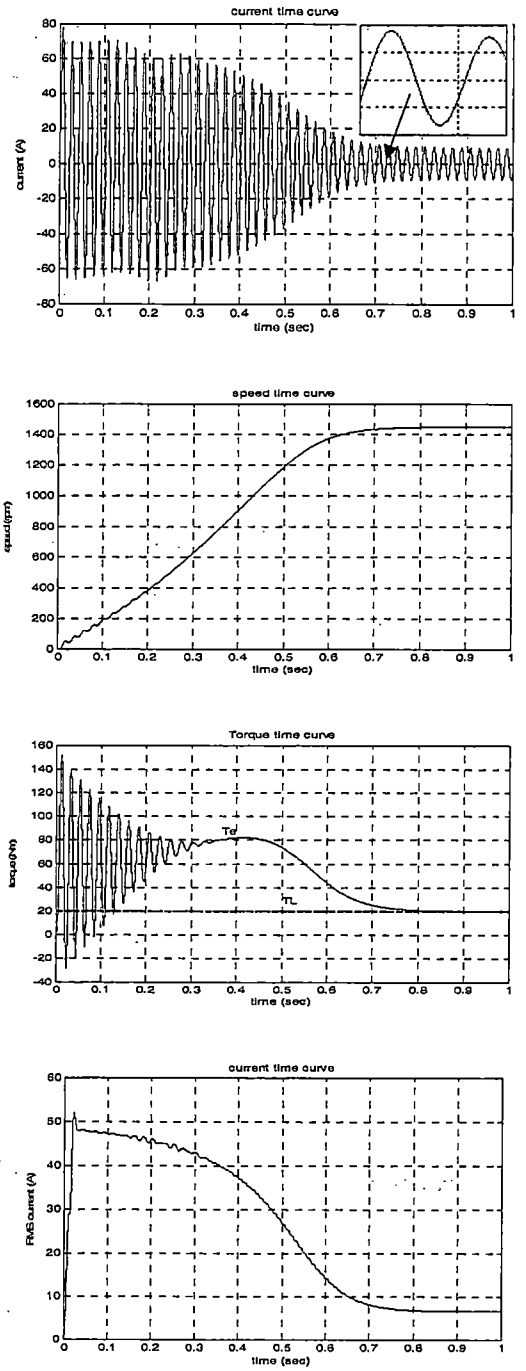

Fig.(3), Transient current, Speed,Torque , and RMS current vs time for balanced sinusoidal operation at constant load application.

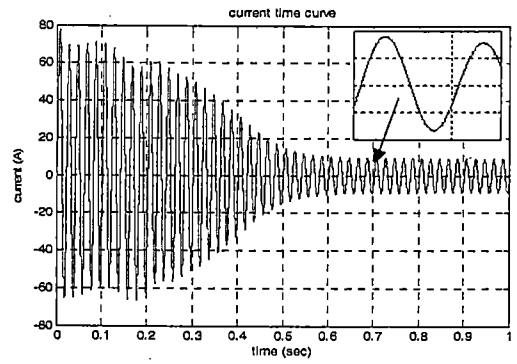

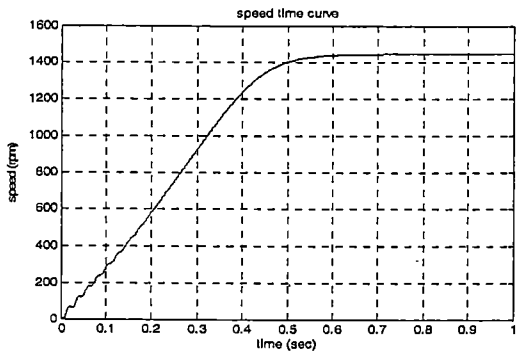

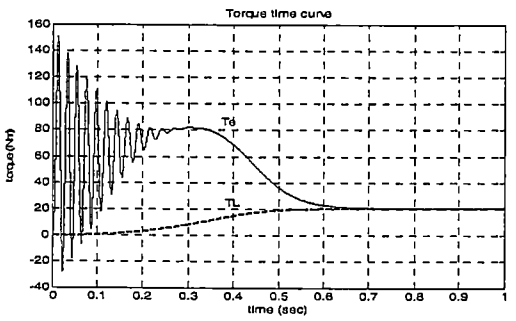

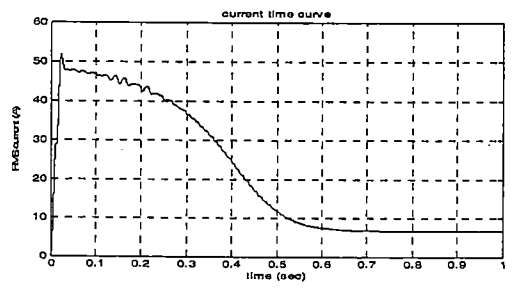

Fig.(4), Transient current, Speed,Torque , and RMS current vs time for balanced sinusoidal operation at pump load application.

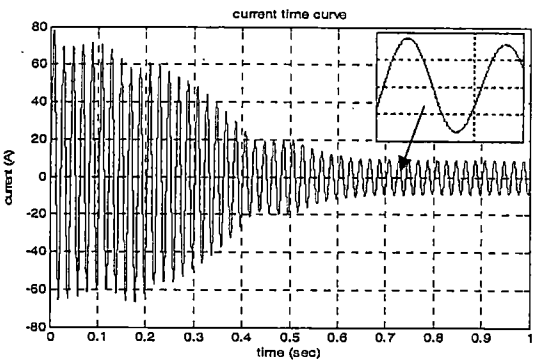

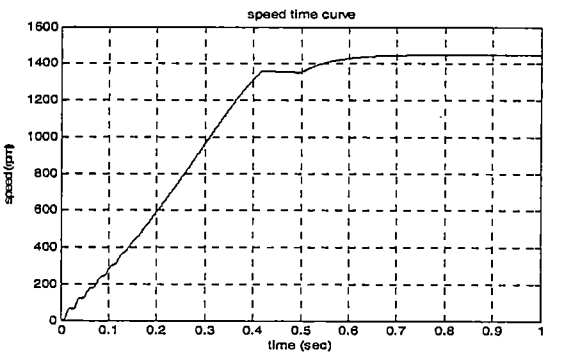

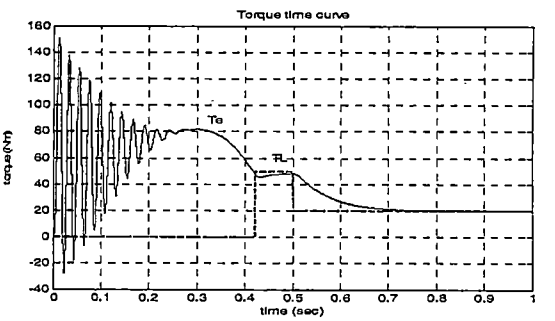

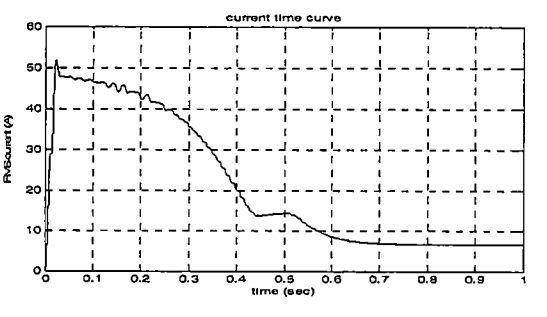

Fig.(5), Transient current, Speed,Torque , and RMS current vs time for balanced sinusoidal operation at pulsed load application.

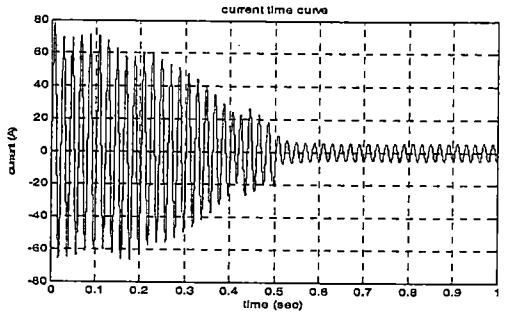

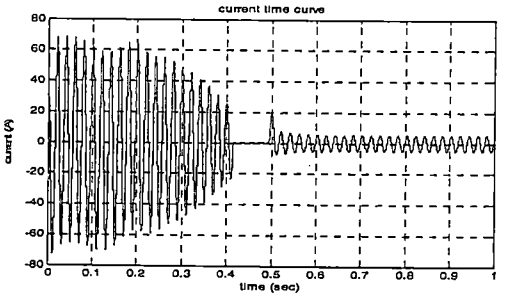

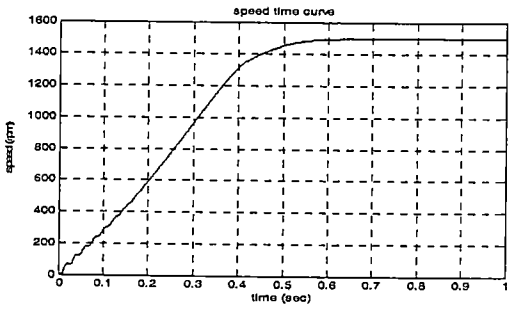

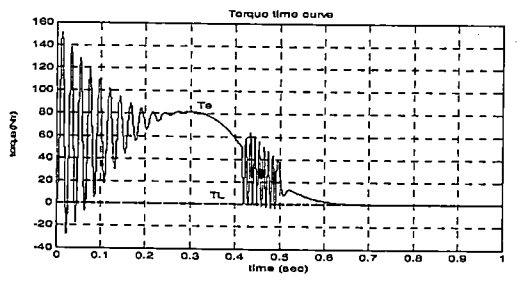

Fig.(6),Transient current of phase-a and phase-c, Speed, and Torque vs time for unbalanced sinusoidal operation at no- load application.

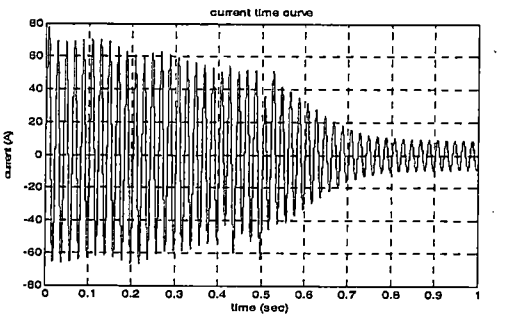

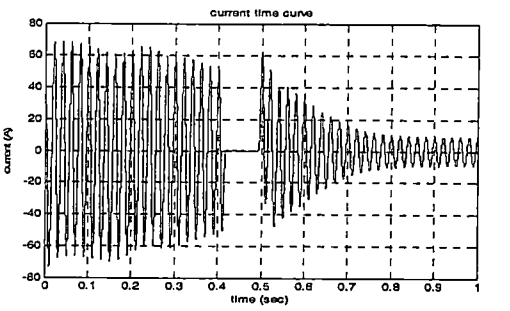

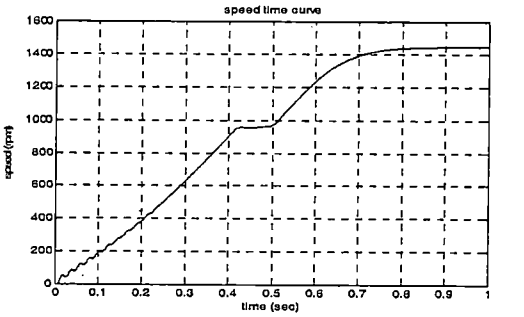

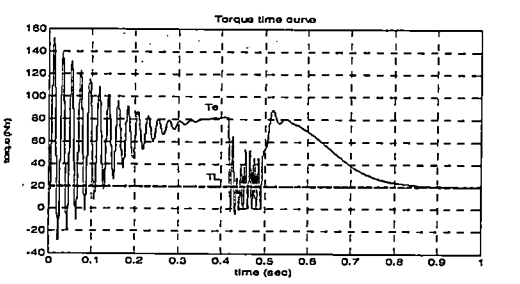

Fig.(7),Transient current of phase-a and phase-c, Speed, and Torque vs time for unbalanced sinusoidal operation at constant load application.

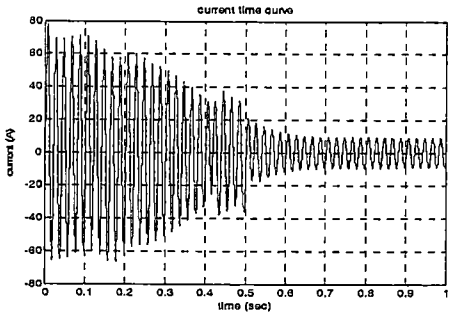

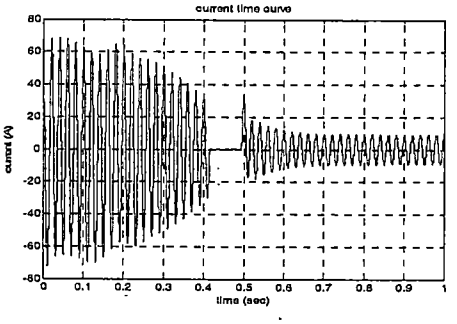

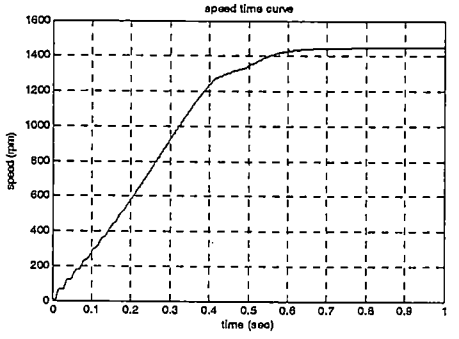

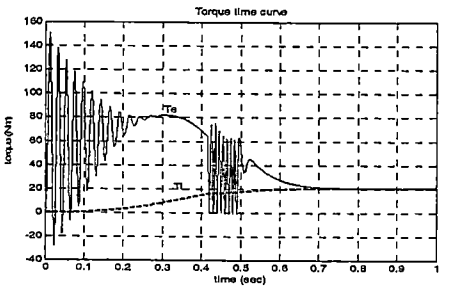

Fig.(8),Transient current of phase-a and phase-c, Speed, and Torque vs time for unbalanced sinusoidal operation at pump load application.

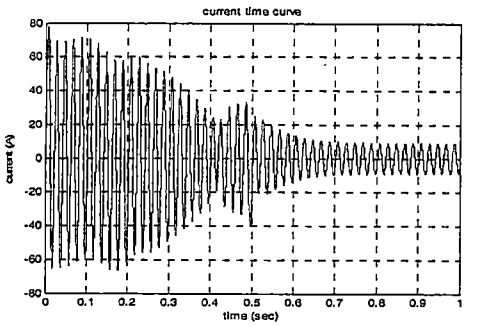

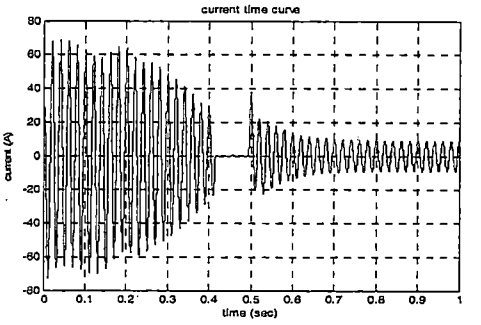

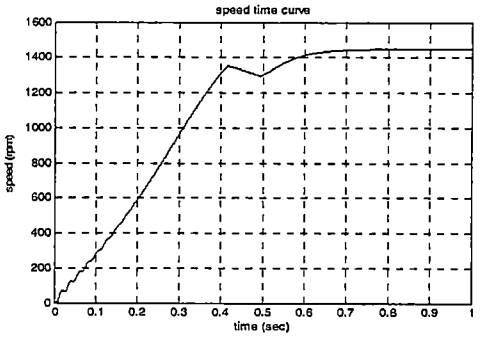

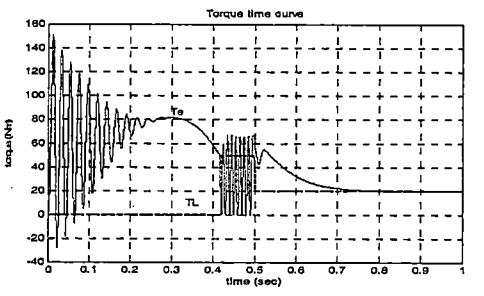

Fig.(9),Transient current of phase-a and phase-c, Speed, and Torque vs time for unbalanced sinusoidal operation at pulsed load application.

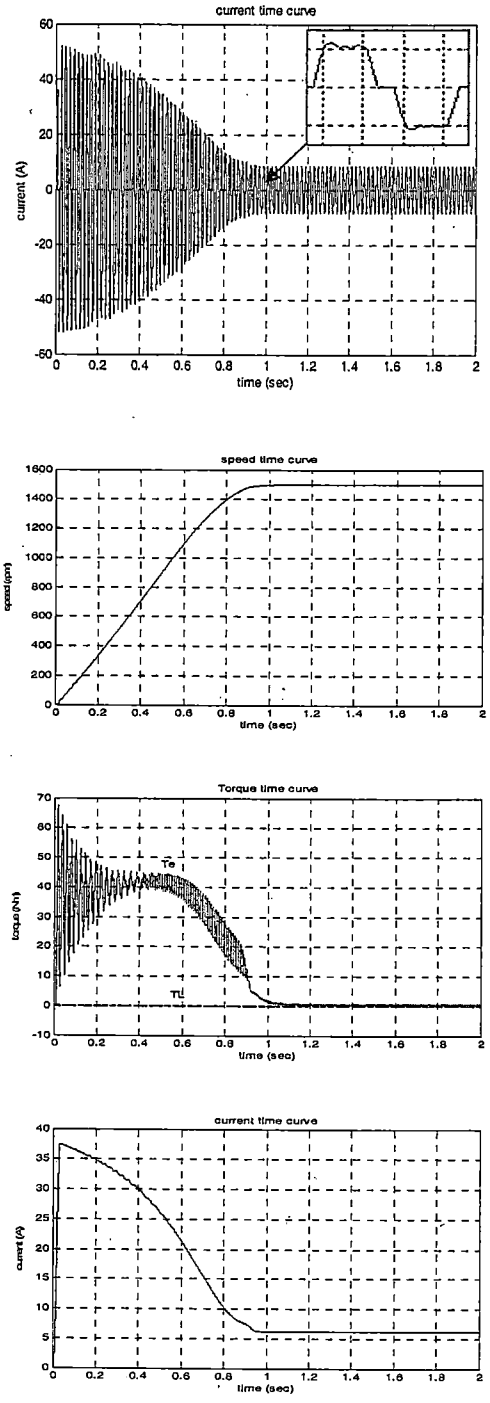

Fig.(10), Transient current, Speed,Torque , and RMS current vs time for balanced non-sinusoidal operation at no- load application. (three-leg thyristorized IM)

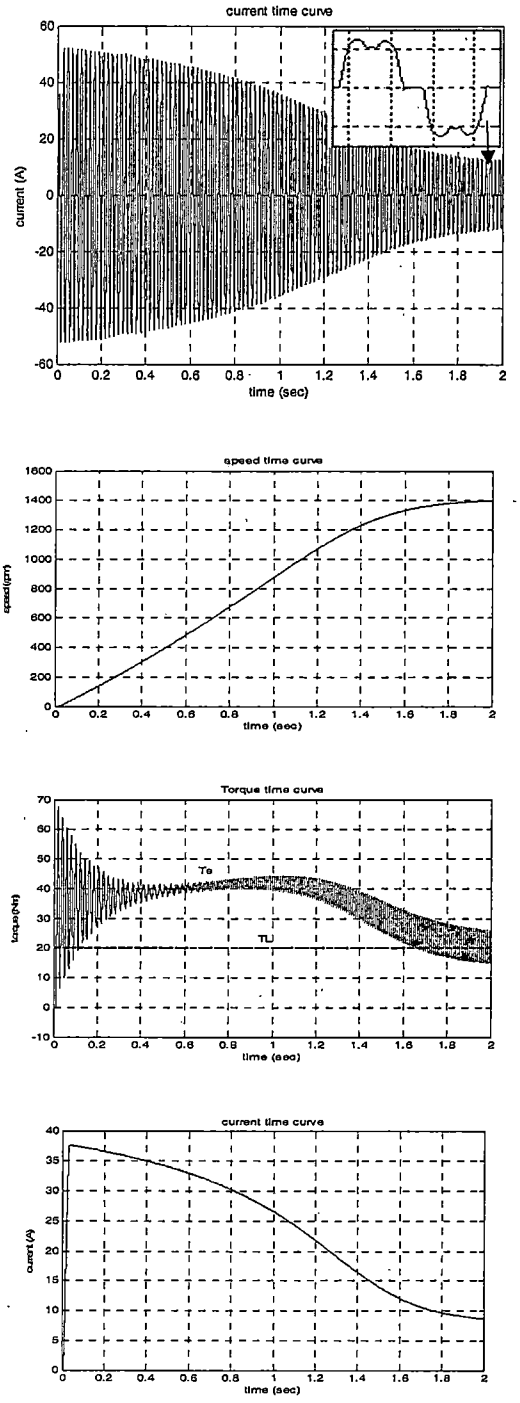

Fig.(11), Transient current, Speed,Torque , and RMS current vs time for balanced non-sinusoidal operation at constant load application. (three-leg thyristorized IM)

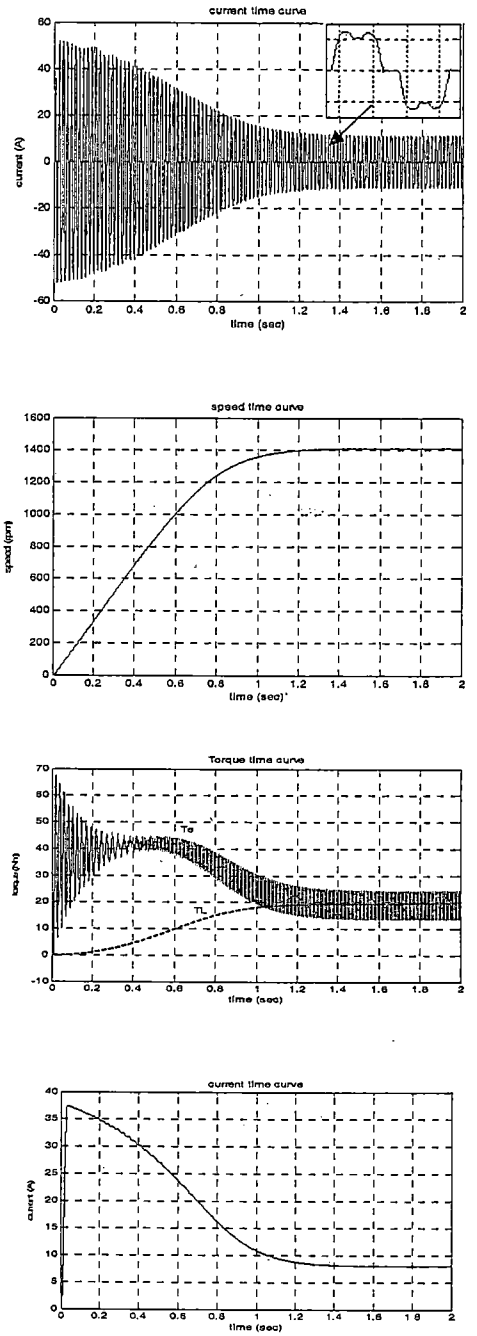

Fig.(12), Transient current, Speed,Torque , and RMS current vs time for balanced non-sinusoidal operation at pump load application. (three-leg thyristorized IM)

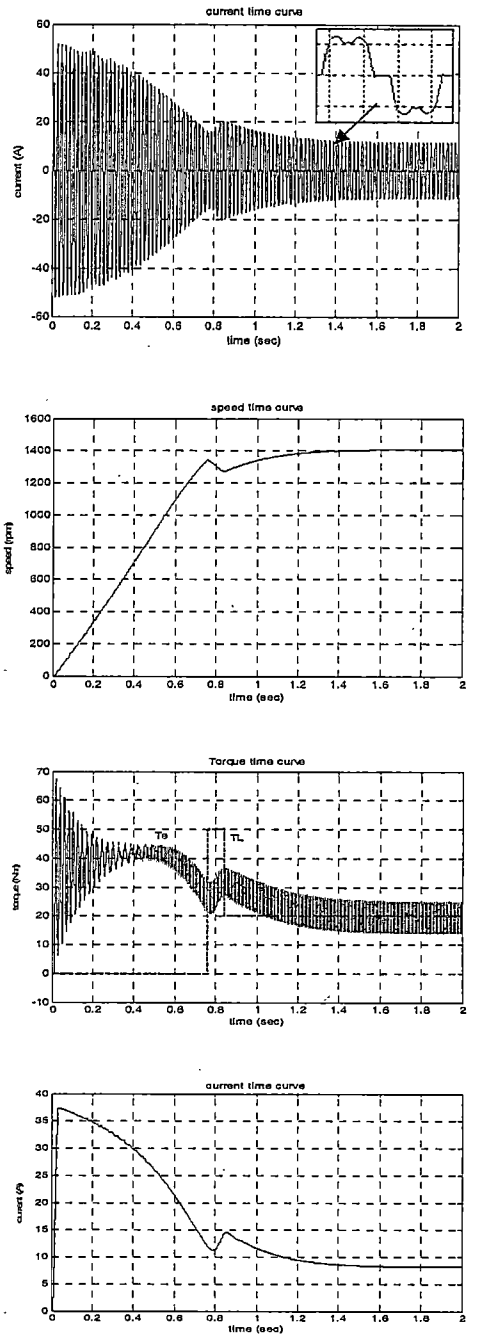

Fig.(13), Transient current, Speed,Torque , and RMS current vs time for balanced non-sinusoidal operation at pulsed load application. (three-leg thyristorized IM)

In the unbalanced operation of thyristorized IM, two distinct types of unbalanced conditions considered in this work are: (1) short-circuit thyristor fault, it can happen in situations such as loose wire in the circuit or breakdown in the snubber circuit, and (2) open-circuit thyristor fault occurring only in one phase of thyristor-controlled three-phase IM, it can occur due to malfunctions either in the gate driver or the pulse generator of the controller . During a short-circuit thyristor fault, the motor terminal of phase-c is connected directly to the supply as shown in Fig.14-a. As a consequence, the problem of voltage unbalances impressed upon the motor windings. This is due to the fact that the motor phase winding without the thyristor connection experiences a full applied voltage at its terminal, whereas the other two phases experience reduced voltages impressed upon them. Fig.15, Fig.16, Fig.17 and Fig.18 show the dynamic performance of motor electromagnetic torque, speed and supply currents when continuous short –circuit thyristor of phase-c fault occurs at which the IM is connected to a three-phase sinusoidal supply through thyristors connected in series with two phases, and the last phase is connected directly to the supply (two-leg thyristorized IM).

During an open-circuit fault in the thyristor switches, both the thyristor switches of phase-c are inactive as shown in Fig.14-b.

Fig.19, Fig.20, Fig.21 and Fig.22 shows the dynamic characteristics of the induction motor when the phase c of the induction motor is disconnected from the supply at the same speed of disconnection time in the case of sinusoidal operation due to open-circuit thyristor fault and then reconnected after five cycles from the disconnection time.

Fig.23, Fig.24, Fig.25 and Fig.26 show the dynamic characteristics of the induction motor when the phase c of the induction motor is connected directly to the supply at the same speed of disconnection time in the case of sinusoidal operation due to short-circuit thyristor fault and then reconnected to the supply through thyristors after five cycles from the disconnection time. .

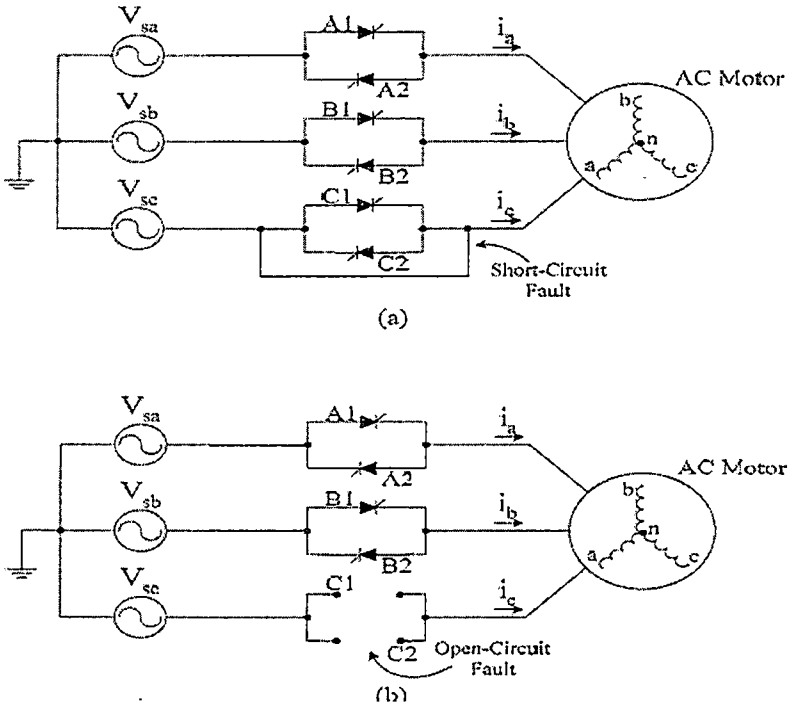

Fig.14. Two types of unbalanced conditions a) short-circuit thyristor fault, b) open-circuit thyristor fault

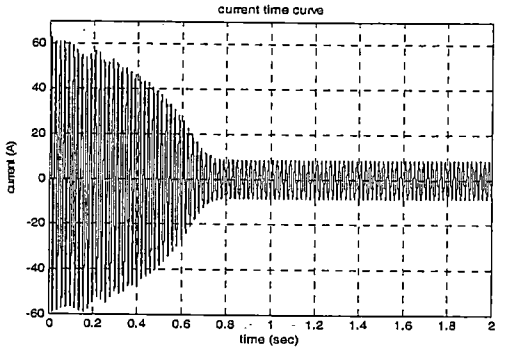

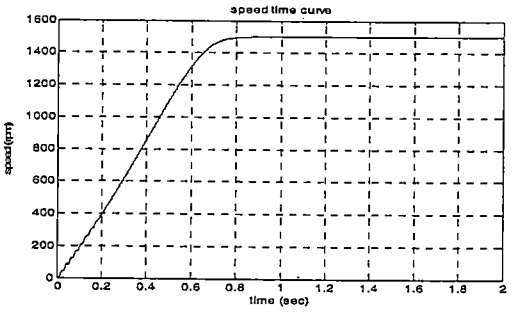

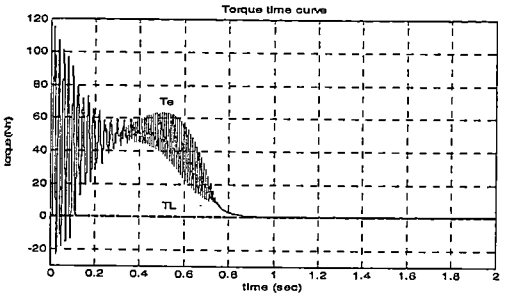

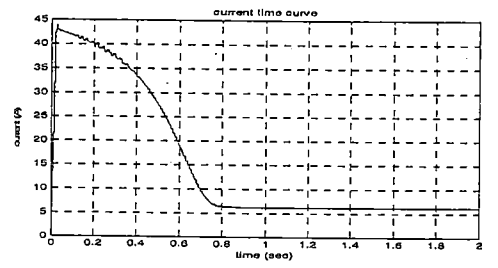

Fig.(15), Transient current, Speed,Torque , and RMS current of phase-a vs time for unbalanced non-sinusoidal operation at no-load application.(two-leg thyristorized IM)

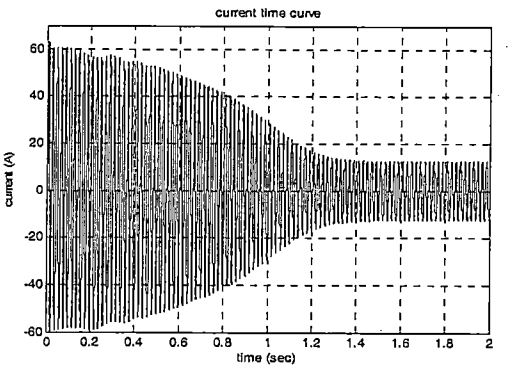

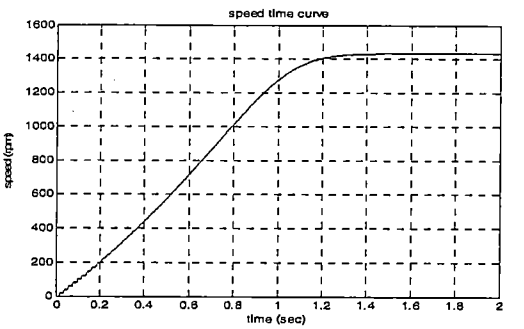

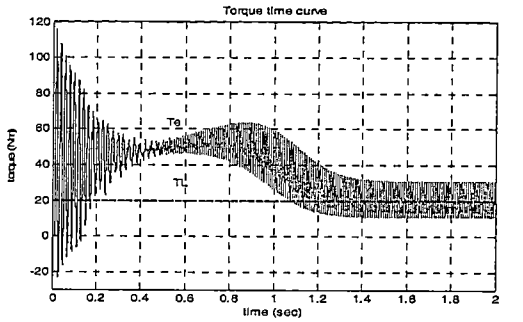

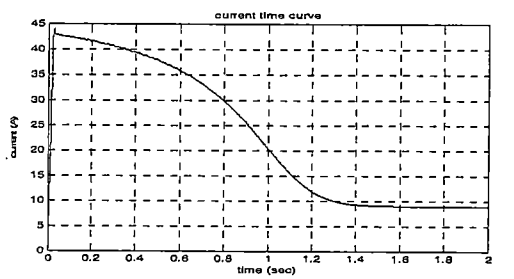

Fig.(16), Transient current, Speed,Torque , and RMS current of phase-a vs time for unbalanced non- sinusoidal operation at constant load application. (two-leg thyristorized IM)

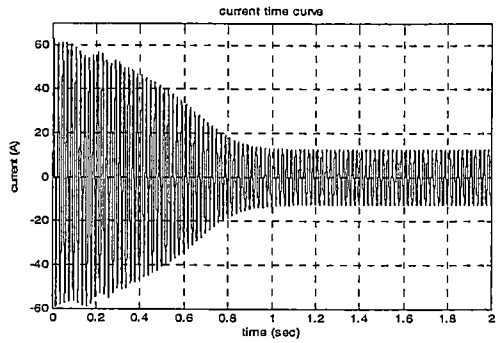

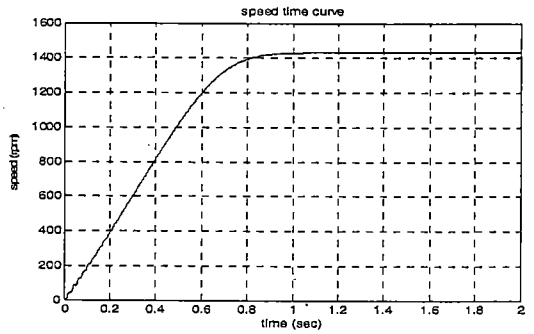

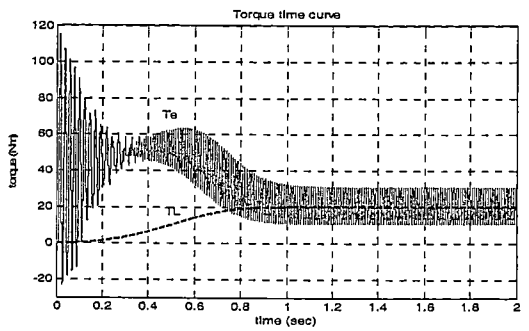

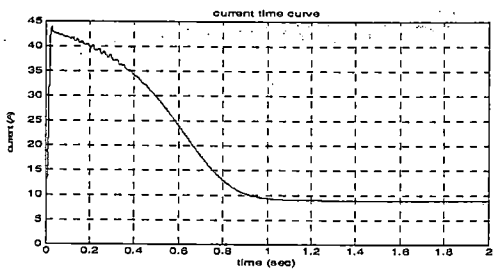

Fig.(17), Transient current, Speed,Torque , and RMS current of phase-a vs time for unbalanced non-sinusoidal operation at pump load application. (two-leg thyristorized IM)

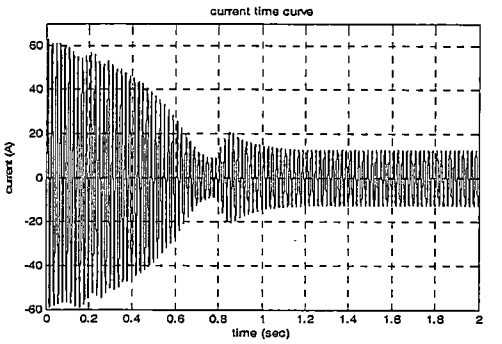

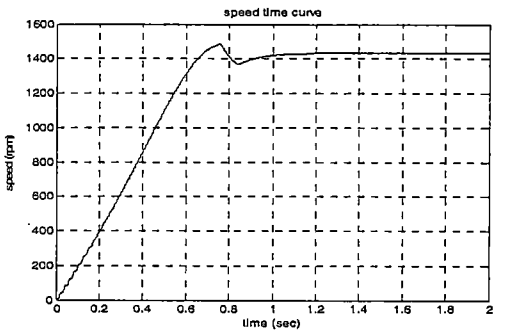

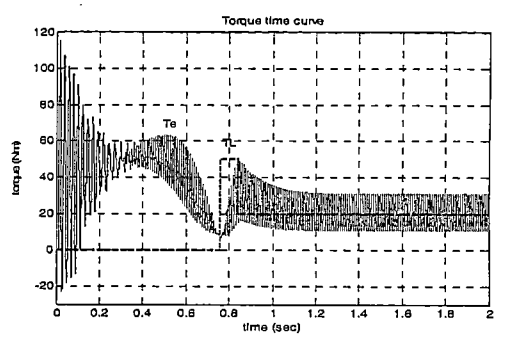

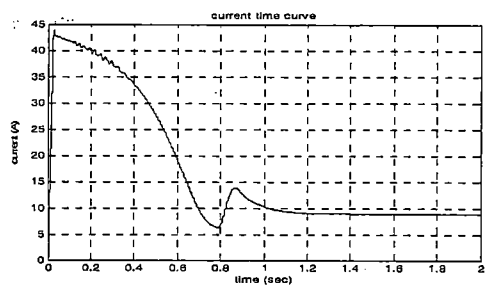

Fig.(18), Transient current, Speed,Torque , and RMS current of phase-a vs time for unbalanced non-sinusoidal operation at pulsed load application. (two-leg thyristorized IM)

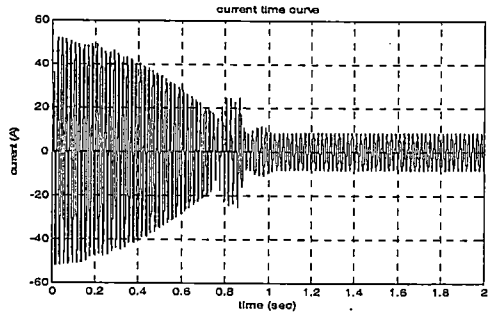

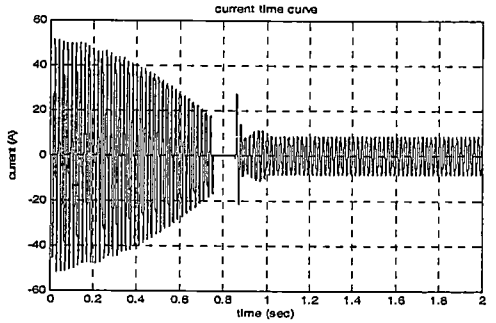

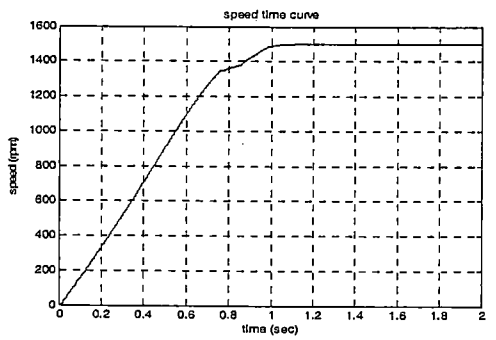

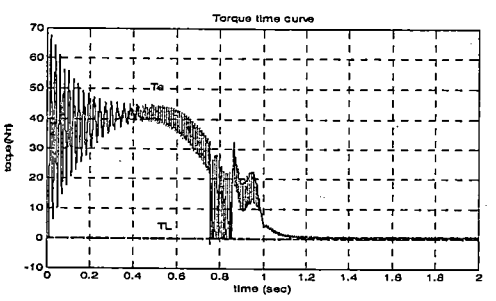

Fig.(19),Transient current, Speed, and Torque vs time for unbalanced non-sinusoidal operation (open-circuit thyristor fault) at no-load application.

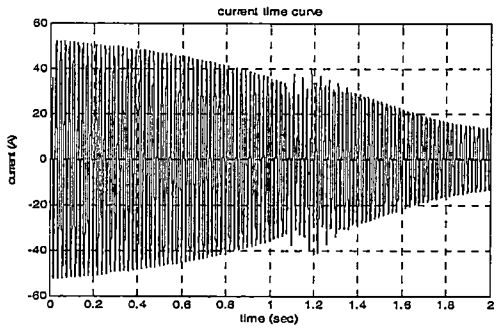

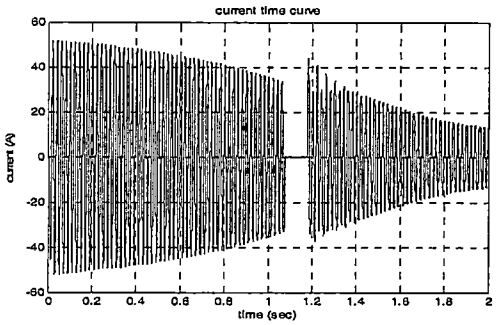

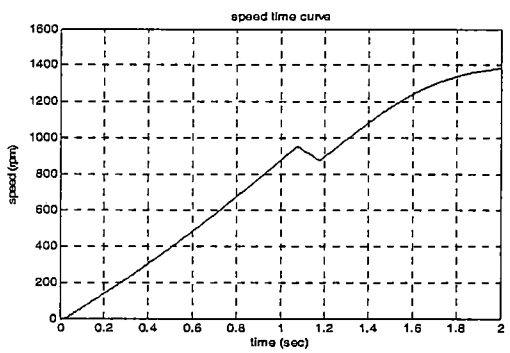

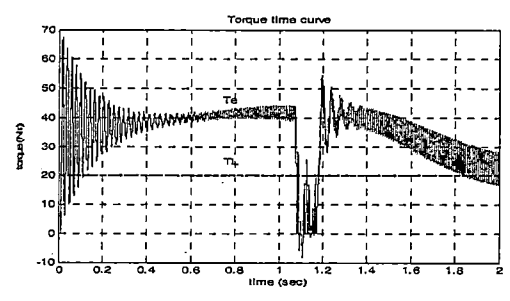

Fig.(20),Transient current, Speed, and Torque vs time for unbalanced non-sinusoidal operation (open-circuit thyristor fault) at constant load application.

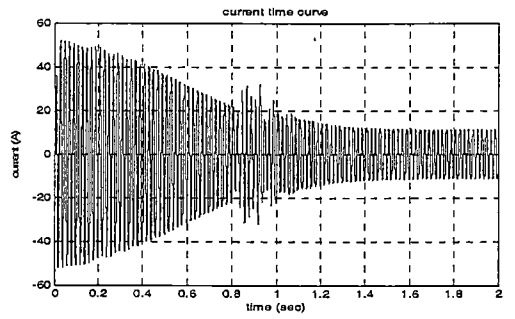

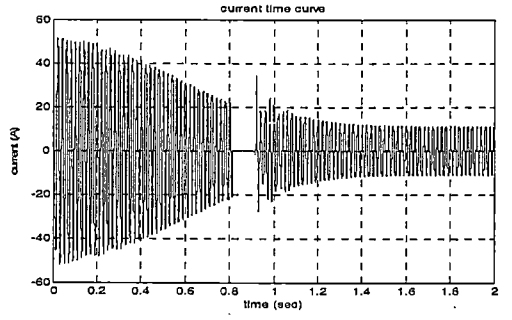

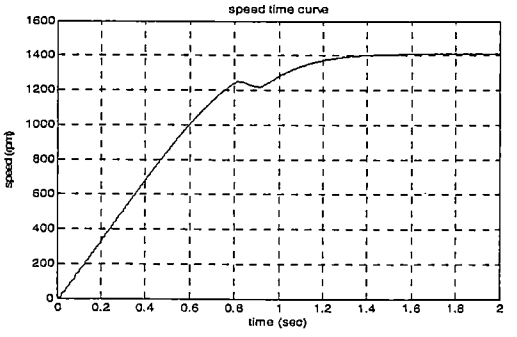

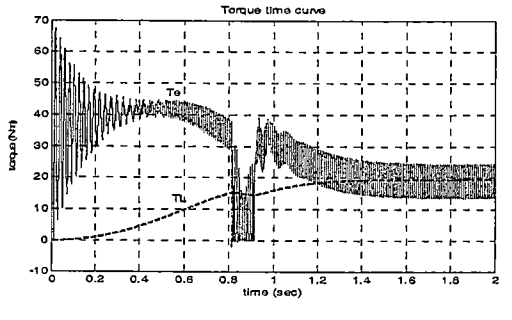

Fig.(21),Transient current, Speed, and Torque vs time for unbalanced non-sinusoidal operation (open-circuit thyristor fault) at pump load application.

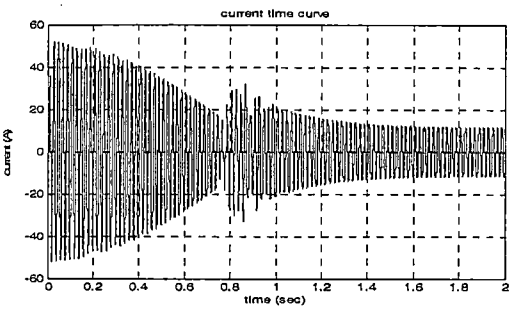

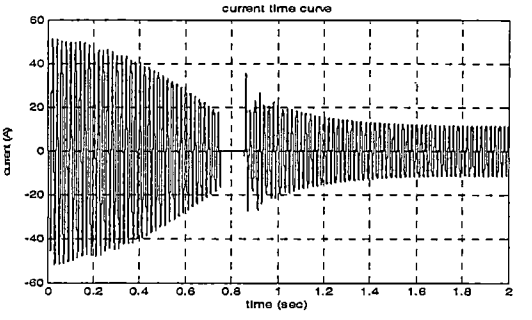

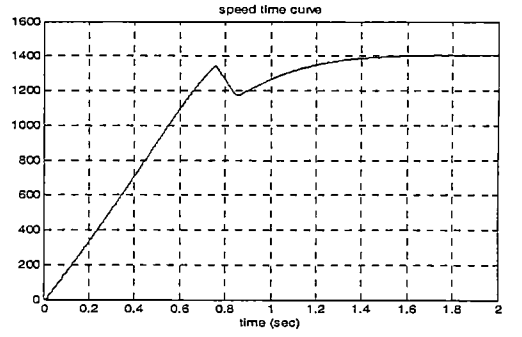

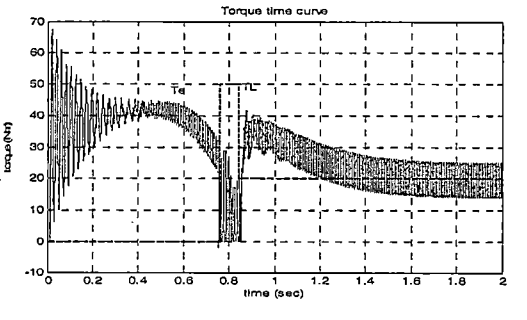

Fig.(22),Transient current, Speed, and Torque vs time for unbalanced non-sinusoidal operation (open-circuit thyristor fault) at pulsed load application.

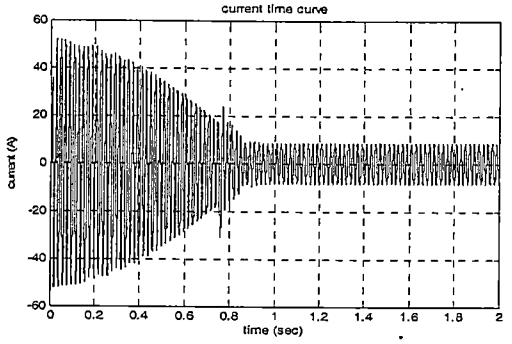

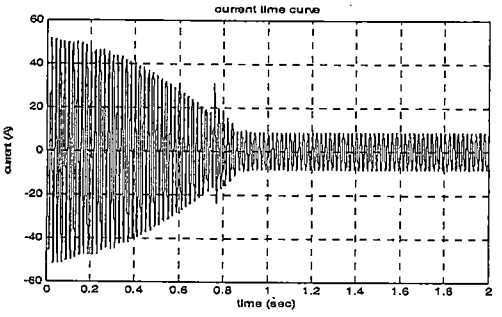

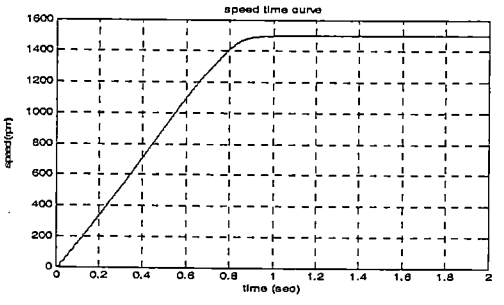

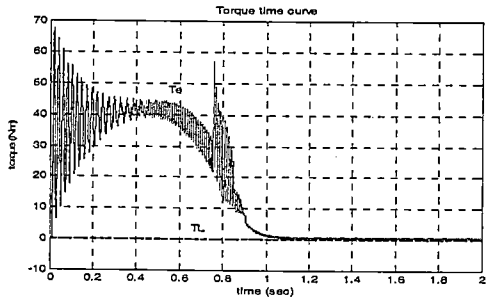

Fig.(23),Transient current, Speed, and Torque vs time for unbalanced non-sinusoidal operation (short-circuit thyristor fault) at no-load application.

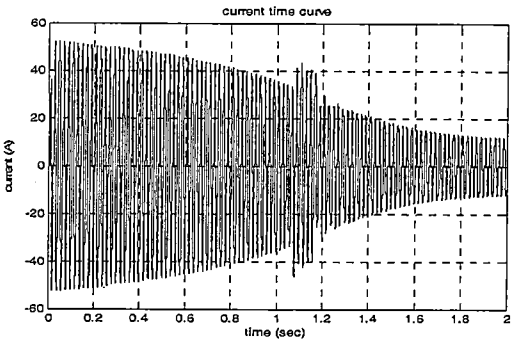

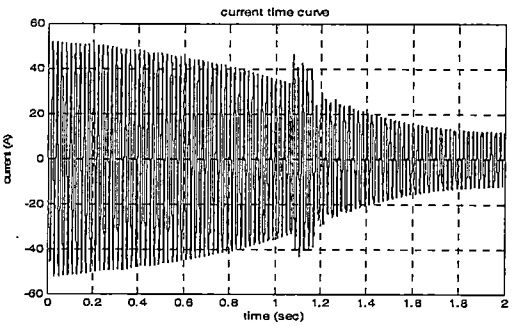

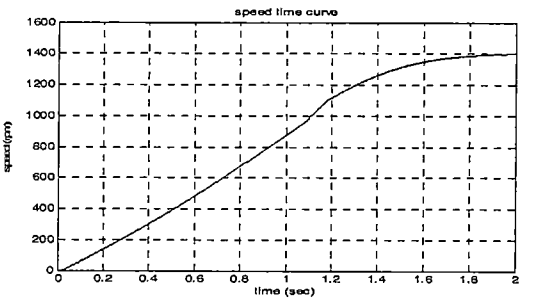

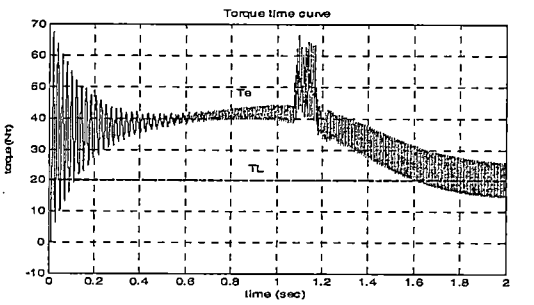

Fig.(24),Transient current, Speed, and Torque vs time for unbalanced non-sinusoidal operation (short-circuit thyristor fault) at constant load application.

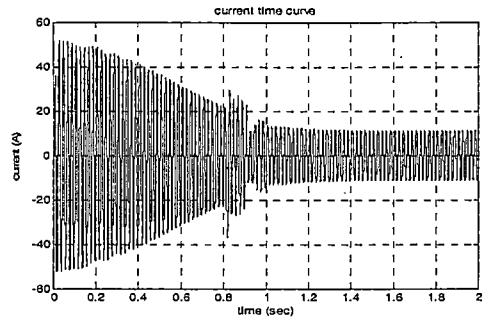

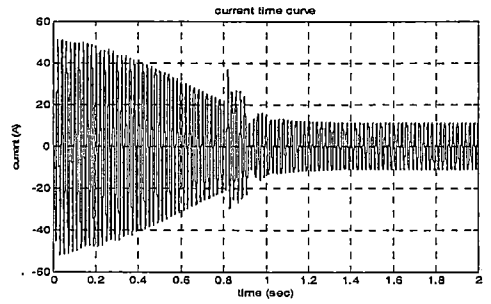

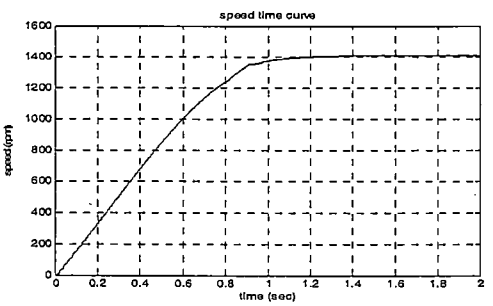

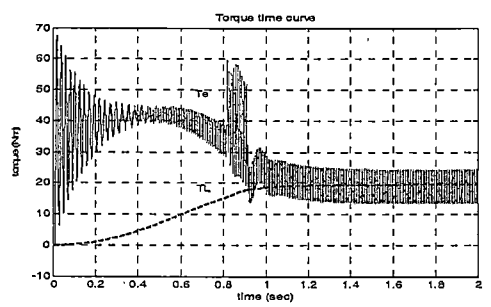

Fig.(25),Transient current, Speed, and Torque vs time for unbalanced non-sinusoidal operation (short-circuit thyristor fault) at pump load application.

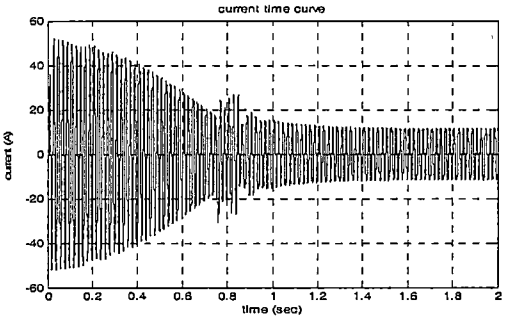

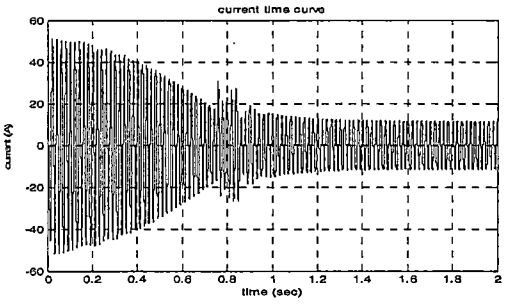

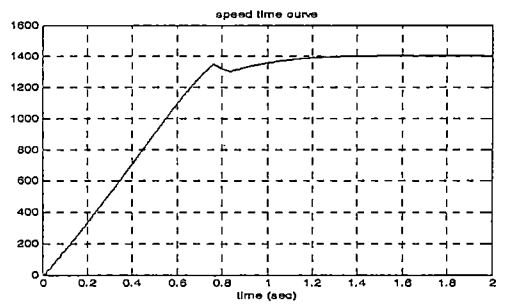

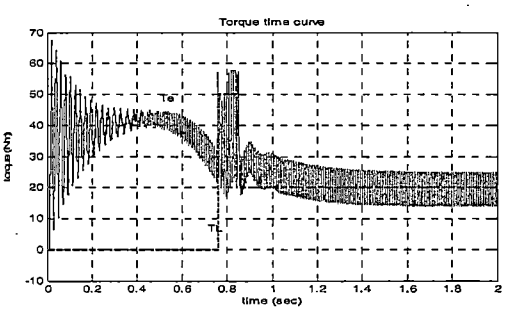

Fig.(26),Transient current, Speed, and Torque vs time for unbalanced non-sinusoidal operation (short-circuit thyristor fault) at pulsed load application.

TABLE I:Sinusoidal IM operation under different loading types

		peak current	Acceleration time	+ve peak torque/ -ve peak torque	RMS starting current
Free acceleration	Balanced	79	0.63	145/30	52
	Unbalanced	79	0.65	145/30	52
Constant load	Balanced	79	0.79	145/30	52
	Unbalanced	79	0.88	145/30	52
Pump load	Balanced	79	0.65	145/30	52
	Unbalanced	79	0.7	145/30	52
Pulsed load	Balanced	79	0.72	145/30	52
	Unbalanced	79	0.75	145/30	52

TABLE II: thyristorized IM operation under different loading types

		peak current	Acceleration time	+ve peak torque/ -ve peak torque	RMS starting current
Free acceleration	Three-leg connection	50	1.1	68/0	37
	Two-leg connection	60	0.9	115/20	44
	O.C thyristor fault	50	1.15	68/0	37
	S.C thyristor fault	50	1.05	68/0	37
Constant load	Three-leg connection	50	2.2	68/0	37
	Two-leg connection	60	1.5	115/20	44
	O.C thyristor fault	50	2.4	68/0	37
	S.C thyristor fault	50	2.05	68/0	37
Pump load	Three-leg connection	50	1.4	68/0	37
	Two-leg connection	60	1.05	115/20	44
	O.C thyristor fault	50	1.7	68/0	37
	S.C thyristor fault	50	1.4	68/0	37
Pulsed load	Three-leg connection	50	1.6	68/0	37
	Two-leg connection	60	1.2	115/20	44
	O.C thyristor fault	50	1.75	68/0	37
	S.C thyristor fault	50	1.5	68/0	37

VI-Disscussion

At the instant of starting of IM, as one can see in the simulation results, the air-gap torque is momentarily increased; reaches positive maximum value, then negative maximum value, and then oscillates about a positive average value. The oscillations in the air-gap torque are caused by the interactions between the stator and rotor flux linkage. The negative oscillations in the electromagnetic torque of the induction motor are presented at the beginning of the start-up period. These are periods of momentary deceleration that occur during regeneration when the electromagnetic torque becomes negative. The rotor speed only increases when the torque is positive. The oscillations that are present in transient of air-gap torque of the induction motor are damped at the end of start up period and finally the steady state condition is attained without oscillations. the oscillations are longer presented in case of bigger load torque on the motor shaft. The response of the air-gap torque is in accordance with the response of the motor currents. the starting current of an induction motor is large , several times larger than the rated current since the back emf induced by Faraday's law grows smaller as the rotor speed increases.

The initial part of the transients of electromagnetic torque and current at the starting , as one can see in the simulation result and tables I,II, is equal in both cases (load and no-load condition) but the acceleration time in case of load condition is longer than in case of no-load condition. In addition the acceleration time is longer When the bigger load torque on the motor shaft is applied. Also decreasing the terminal voltage causes longer acceleration time.

From Tables I,II, it was observed that thyristorized IM affects the following aspects.

1)-It reduces the inrush current drawn by the motor.

2)- It has significant effects on the motor electromagnetic torque during starting period in which the negative torque pulsation is disappeared and the positive torque pulsation is reduced so the torque pulsations decrease.

3)-Speed build up is found to be smooth since the torque pulsations is reduced.

4)- It results into a high acceleration time , where as it is largely increasing with constant load application .

In the unbalanced condition, the simulation result for the case of continuous open-circuit thyristor switch fault is not presented here since the motor does not produce a starting torque during the occurrence of such fault; hence, it constitutes a total failure of motor starting. Also, open-circuit thyristor switch fault for

five cycles cause deceleration of the motor because the average value of electromagnetic torque is lower than the load torque.

During a short-circuit SCR fault, the motor terminal of phase-*c* is connected directly to the utility grid, as a consequence, the problem of voltage unbalances impressed upon the motor windings arises during starting. This is due to the motor phase winding without the SCR connection experiences a full applied voltage, whereas the other two phases experience reduced voltages impressed upon them during starting. the voltage unbalances introduce a negative sequence components in the stator currents, which consequently lead to average torque reduction and torque pulsations during the starting transients since it produces a negative torque opposite to the motor's rotation.

Also from the simulation results, It is noted that the short-circuit thyristor switch fault produces undesired fault response on motor performance with unbalanced, high motor currents, which accordingly imposes a greater stress on the motor windings.

VII-Conclusion

This paper presents the dynamic performance of IM under different supply voltage waveforms and different loading types. And it is observed that the dynamic performance of IM is greatly affected by changes in its supply voltage and load types.

In this paper, It is investigated that

1-the peak torque and current at the starting are independent of the load value and its type but depend upon the motor terminals voltage.

2- The oscillations of the transient torque depend upon the load .they are longer in case of bigger load torque on the motor shaft.

3-The average of the transient torque depend upon the value of the load and its type and the motor terminal voltage.

4- The acceleration time depends upon the load type, its value, and the motor terminals voltage.

5-The unbalanced supply voltage produces undesired response on motor performance with unbalanced, high motor currents, which accordingly result in high motor transient torque pulsations and long acceleration time.

REFERENCES

[1] P. C. Krause and C. H. Thomas, "Simulation of symmetrical induction machinery," IEEE Trans. Power App. Syst., vol. PAS-84, no. 11, pp. 1038–1053, Nov. 1965.

[2] A. K. DeSarkar and G. J. Berg, "Digital simulation of three-phase induction motors," IEEE Trans. Power App. Svst., vol. 89, pp.1031-1037, 1970.

motor", IEEE *Transactions on Energy Conversion*, Vol. 14, No.2. 193-201, 1999.

[4] J.Tegopoulos, "Analysis of supply voltage distortion effects on induction motor operation", IEEE *Transactions on Energy Conversion*, Vol. 16, pp. 209-213, 2001.

[5] W. Deleroi, J. B.Woudstra, and A. A. Fahim, "Analysis and application of three-phase induction motor voltage controller with improved transient performance," *IEEE Trans. Ind. Appl.*, vol. 25, no. 2, pp. 280–286, Mar./Apr. 1989.

[6] T. M. Rowan and T. Lipo, "A quantitative analysis of induction motor performance improvement by SCR voltage control," *IEEE Trans. Ind. Appl.*, vol. IA-19, no. 4, pp. 545–553, Jul./Aug. 1983.

[7] S. A. Hamed and B. J. Chalmers, "Analysis of variable-voltage thyristor controlled induction motors," *Proc. Inst. Elect. Eng.*, pt. B, vol. 137, no. 3, pp. 184–193, May 1990.

[8] Lipo T.A., 1971b. The analysis of induction motors with voltage control by symmetrically triggered thyristors, *IEEE Trans. On Power Apparatus and Systems,* Vol. PAS-90, No. 2, pp. 515-525.

[9] A.Amin , "Numerical computation concerning the influence of a stator-side thyristor-controlled on the squirrel cage induction motor performance" UPEC 85,Hudders-field,England,1984.

[10] J. Faiz, M. Ghaneei, A. Keyhani, "Performance analysis of fast re-closing transients in induction motors", IEEE *Transactions on Energy Conversion*, Vol. 14, pp. 101-107, 1999.

[11] R.T. Ugale, B.N. Chaudhari, "Effect of short power interruptions on performance of AC motors" Industrial Technology, 2012. ICIT 2012. IEEE International Conference.

[12] Eltamaly A.M., Alolah A.I. and Hamouda R.M., 2007a. Performance evaluation of three-phase Induction motor under different AC voltage control strategies: Part 1, *Proc. Int. Applied Electric Machine and Power Electronics ACEMP '07,* pp.770-774, 10 Sept. 2007.

[13] Eltamaly A.M., Alolah A.I. and Hamouda R.M., 2007b. Performance Evaluation of three-phase Induction motor under different AC voltage control strategies 'Part II, *Proc. Int. Applied Electric Machine and Power Electronics ACEMP '07,* pp. 17-22, 10-12 Sept. 2007

[14] M. Mirošević, "The Dynamics of Induction Motor Fed Directly from the Isolated Electrical Grid", International Journal Of Renewable Energy Research, IJRER, *Vol.1, No3, pp.126-133, 2012.*

[15] S. S. Murthy and G. J. Berg, "A new approach to dynamic modeling and transient analysis for SCR-controlled induction motors," IEEE Trans. Power

App. Syst., vol. PAS-101, no. 9, pp. 3141–3150, Sep. 1982.

[16] G. Nath and G. J. Berg, "Transient analysis of three-phase S.C.R. controlled induction motors," IEEE Trans. Ind. Appl., vol. IA-17, no. 2, pp. 133–142, Mar./Apr. 1981.

[17] P. C. Krause, O. Wasynczuk, and S. D. Sudhoff, Analysis of Electric Machinery and Drive Systems, 2nd ed. New York: Wiley, 2002.

[18] R.krishnan, Electric Motors Drives, Modeling, Analysis, and control, 2nd ed. New York: Pantice Hall, 2001.

[19] Rockwell Automation, Application basics of operation of three-phase induction motors,(1996).

[20] J. Faiz, M. Ghaneei, A. Keyhani, "Performance Optimization of Induction Motors During Voltage-Controlled Soft Starting", IEEE *Transactions on Energy Conversion*, Vol. 19, 2004.

[21] TheMathWorks, Inc., Natick,MA. Matlab, . version 9.1. (2011). [Online].Available: http://www.mathworks.com.

APPENDIX (A): (MOTOR DATA)

Rs = 1.405 Ω; R'r = 1.395 Ω;

Lls = 0.005839H; L'lr = 0.005839H;

Lm = 0.1722 H;

pole = 4; rated voltage = 380 V;

rated power = 3 kW; rated current = 7 A;

winding connection = Wye;

rated frequency = 50 Hz;

total inertia = 0.203 kg · m2 ;

rated speed = 1440 r/min.

NOMENCLATURE

r Rotor quantity

s Stator quantity

R_s, L_{ls} Stator resistance and leakage inductance

L_m Magnetizing inductance

L_s Total stator inductance

v_{abcs}, i_{abcs} stator voltages and currents

ω_m Mechanical angular velocity of the rotor

Θ_m Rotor angular position

P Number of poles.

ω_r Electrical angular velocity ($\omega_m \times P/2$)

Θ_r Electrical rotor angular position ($\Theta_m \times P/2$)

T_e Electromagnetic torque

T_m Shaft mechanical torque

J Combined rotor and load inertia coefficient.

F Combined rotor and load friction coefficient

L'_r Total rotor inductance

R'_r, L'_{lr} Rotor resistance and leakage inductance

v_{abcr}, i_{abcr} rotor voltage and current